HEALTH AND MEDICINE

Exosome-based delivery of super-repressor IκBα relieves sepsis-associated organ damage and mortality

Hojun Choi[1,2]*, Youngeun Kim[3]*, Amin Mirzaaghasi[1], Jaenyoung Heo[3], Yu Na Kim[3], Ju Hye Shin[4], Seonghun Kim[5], Nam Hee Kim[6], Eunae Sandra Cho[6], Jong In Yook[6], Tae-Hyun Yoo[5], Eunjoo Song[7], Pilhan Kim[2,7,8], Eui-Cheol Shin[2†], Kyungsoo Chung[4†], Kyungsun Choi[3†], Chulhee Choi[1,2,3]

As extracellular vesicles that play an active role in intercellular communication by transferring cellular materials to recipient cells, exosomes offer great potential as a natural therapeutic drug delivery vehicle. The inflammatory responses in various disease models can be attenuated through introduction of super-repressor IκB (srIκB), which is the dominant active form of IκBα and can inhibit translocation of nuclear factor κB into the nucleus. An optogenetically engineered exosome system (EXPLOR) that we previously developed was implemented for loading a large amount of srIκB into exosomes. We showed that intraperitoneal injection of purified srIκB-loaded exosomes (Exo-srIκBs) attenuates mortality and systemic inflammation in septic mouse models. In a biodistribution study, Exo-srIκBs were observed mainly in the neutrophils, and in monocytes to a lesser extent, in the spleens and livers of mice. Moreover, we found that Exo-srIκB alleviates inflammatory responses in monocytic THP-1 cells and human umbilical vein endothelial cells.

INTRODUCTION

Sepsis is a systemic inflammatory syndrome caused by activation of the innate immune system due to acute microbial infection. It continues to be the main cause of mortality in intensive care units, with an estimated 400,000 to 600,000 patients developing sepsis annually in the US and Europe (*1*). On September 13 of each year, "World Sepsis Day" is published by the Global Sepsis Alliance. Sepsis is a serious disease that has become a major social issue. Previously, Xigris (Eli Lilly) was introduced in 2001 as the only U.S. Food and Drug Administration–approved sepsis treatment; however, it was withdrawn from the market in October 2011 due to bleeding-related side effects and lack of efficacy (*2*). Currently, no sepsis-specific treatments are available for clinical usage. The development of effective alternative therapies for sepsis is urgently needed.

Uncontrolled inflammation is a prominent feature of the septic response (*3*, *4*). Host-pathogen interactions mediated by Toll-like receptors stimulate the production of proinflammatory cytokines, chemokines, and immune-activating molecules (*5*). This proinflammatory response is followed by a compensatory immunosuppressive response that involves various quantitative and functional defects of immune cells. Pathogen-induced cellular modification is accompanied by marked changes in host gene expression (*6*), with nuclear factor κB (NF-κB) transcription factors playing a pivotal role in modulating these changes. Several cytokines under the regulatory control of NF-κB, including tumor necrosis factor–α (TNF-α) and interleukin-1 (IL-1), can induce further activation of this transcriptional factor, leading to potentiation of the inflammatory response and septic shock. In addition, NF-κB is involved in the apoptotic response, primarily through enhancing the transcription of antiapoptotic genes such as Bcl-x_L, A1, and A20 (*7*, *8*). Inflammation associated with NF-κB activation can, thus, be exacerbated by two interacting mechanisms, increased expression of proinflammatory mediators and prolongation of the life spans of cell populations such as neutrophils, which are activated to produce proinflammatory molecules and participate directly in acute inflammatory processes.

Recent studies in animal models of sepsis induced either by lipopolysaccharide (LPS; endotoxin model) or cecal ligation and puncture (CLP; polymicrobial model) have demonstrated that NF-κB inhibitors with diverse chemical properties and mechanisms of action protect animals from septic lethality (*9*–*12*). Although more than 700 inhibitors of NF-κB have been reported (*13*), no NF-κB blocker has been approved for human use to date. Various steroids and nonsteroid anti-inflammatory drugs have been found to block NF-κB, but their effects are highly pleiotropic and lack specificity. Novel therapeutic strategies aimed at specific inhibition of key elements in the NF-κB activation pathway have been under development in recent years, and expectations are high regarding their potential efficacy as sepsis treatments. Genetic constructs expressing an engineered inhibitor of nuclear factor κBα (IκBα) protein without sites for phosphorylation, super-repressor IκB (srIκB), have also been used. IκBα mutation at specific phosphorylation sites (Ser^{32} and Ser^{36} replaced to Ala) results in a dominant active form of IκBα with a prolonged half-life. These srIκBs lead to a stable cytoplasmic pool of IκBα, thereby preventing nuclear NF-κB activation (*14*, *15*).

Here, we used exosomes as a therapeutic carrier to deliver srIκB to a therapeutic target. Exosomes have been recognized as potent therapeutic vehicles for transferring various proteins and regulatory genes to target cells (*16*–*18*). They function as nonimmunogenic

[1]Department of Bio and Brain Engineering, KAIST, Daejeon 34141, Republic of Korea. [2]Graduate School of Medical Science and Engineering, KAIST, Daejeon 34141, Republic of Korea. [3]ILIAS Biologics Inc., Daejeon 34014, Republic of Korea. [4]Division of Pulmonology, Department of Internal Medicine, Yonsei University College of Medicine, Seoul 03722, Republic of Korea. [5]Department of Internal Medicine, Yonsei University College of Medicine, Seoul 03722, Republic of Korea. [6]Department of Oral Pathology, Oral Cancer Research Institute, Yonsei University College of Dentistry, Seoul 03722, Republic of Korea. [7]IVIM Technology, Daejeon 34051, Republic of Korea. [8]Graduate School of Nanoscience and Technology, KAIST, Daejeon 34141, Republic of Korea.
*These authors contributed equally to this work.
†Corresponding author. Email: kchoi@iliasbio.com (K.Cho.); euicheols@kaist.ac.kr (E.-C.S.); chungks@yuhs.ac (K.Chu.)

nanovesicles and can protect their cargo from serum proteases and immune responses (*19*). Loading of soluble proteins into exosomes has been enabled by a technology called EXPLOR, which exploits the natural exosome biogenesis process and reversible protein-protein interactions controlled by optogenetics (*20*). To load specific target proteins into exosomes, we generated a human embryonic kidney (HEK) 293T cell line that stably expresses two recombinant proteins, CIBN-EGFP-CD9 and srIκB-mCherry-CRY2 (Fig. 1A). Consistent with previous studies, EXPLOR technology was used to produce srIκB-loaded exosomes. We designated the srIκB loading exosomes as Exo-srIκB, and exosomes generated from intact HEK293T cells as Exo-Naïve. By applying Exo-srIκB to sepsis models for therapeutic purposes, we ameliorated sepsis-induced organ injury and inhibited the secretion of proinflammatory cytokines, thereby improving the overall survival of patients with sepsis.

RESULTS

Characterization and analysis of srIκB-loaded exosomes

To produce sufficient exosomes, we collected culture medium from each cell type. Exosomes were isolated using a combination of tangential flow filtration (TFF) and size exclusion chromatography (SEC) (fig. S1A). To reduce the risk of loading the SEC column with impurities that would exceed its binding capacity, the samples were subjected to diafiltration and concentration through TFF. After TFF, the concentrated medium was loaded onto an SEC column for further purification. A second TFF was then performed to concentrate the exosomes. Each type of exosome isolated through sequential purification was analyzed via nanoparticle tracking analysis (NTA), which characterizes the size and concentration of exosomes (fig. S1B). Particles with diameters from 30 to 120 nm accounted for over 80% of all particles, with a mean size of 101 nm, which is consistent with the characteristic size range (30 to 120 nm) of exosomes. In addition, transmission electron microscopy (TEM) showed intact cup-shaped membrane vesicles with sizes corresponding to the NTA results obtained from Exo-Naïve and Exo-srIκB (Fig. 1B). To further characterize the exosomes in our preparations, we investigated two common exosome markers, the tetraspanins CD63 and TSG101, through Western blotting. The presence of CD63 and TSG101 was observed in the samples, whereas a Golgi-derived contaminant, GM130, was only detected in the cell lysate (Fig. 1C). This analysis of the exosome preparations showed that they exhibit the characteristics of exosomes. Furthermore, we observed robust loading of srIκB-mCherry-CRY2 (130 kDa) into exosomes isolated from srIκB stable cell lines.

Exo-srIκB improves survival and ameliorates acute organ injury in septic mice

We investigated whether intraperitoneal injection with Exo-srIκB protected against endotoxic shock. Animals received a single intraperitoneal injection with a lethal dose of LPS (40 mg/kg body weight for C57BL/6, and 20 mg/kg body weight for BALB/c), followed by a single intraperitoneal injection of Exo-srIκB (6 hours apart). Compared with control C57BL/6 mice, which showed 100% mortality

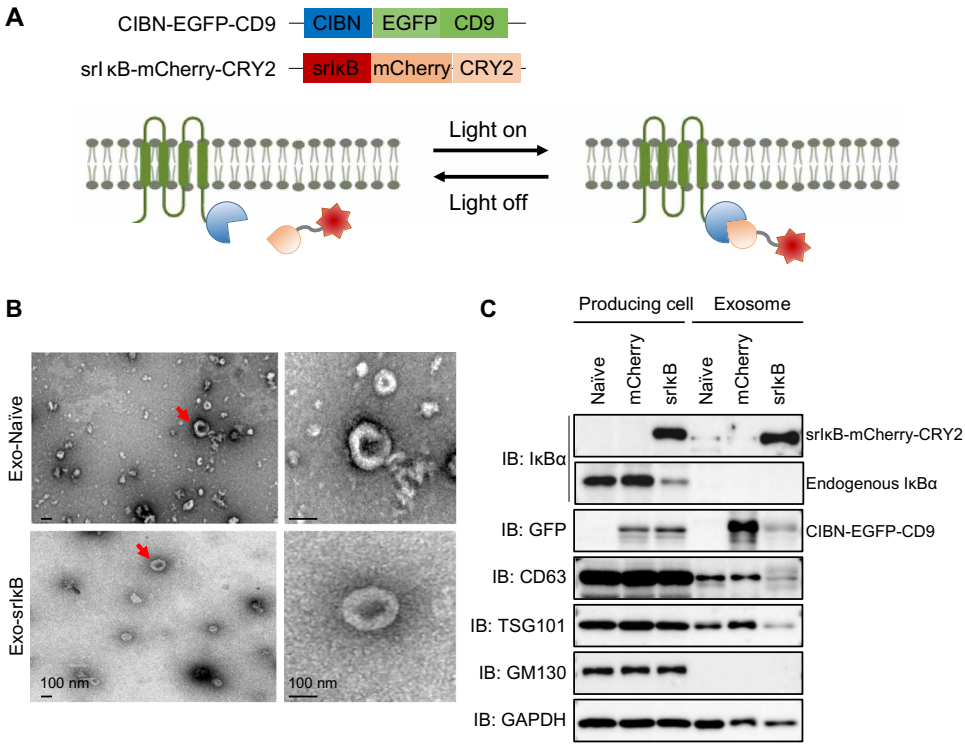

Fig. 1. Generation and characterization of engineered exosomes. (**A**) Schematic of DNA constructs used for the production of Exo-srIκB (top). Schematic showing fusion proteins and their proposed activities (bottom). (**B**) Morphological characterization of Exo-Naïve and Exo-srIκB through transmission electron microscopy. (**C**) HEK293T cells that stably express mCherry or srIκB, and exosomes from these HEK293T cells, were lysed and immunoblotted against the indicated proteins. IB, immunoblot.

due to LPS-induced sepsis, mice treated with Exo-srIκB were remarkably resistant to LPS-induced mortality; most of the mice were rescued from sepsis and showed prolonged survival (Fig. 2A, top). Exo-srIκB–mediated effects were associated with modest protection from the LPS-induced temperature drop (fig. S2A). We also developed a mouse model of LPS-induced sepsis using BALB/c mice. Exo-srIκB treatment significantly improved the survival rate of LPS-induced sepsis in BALB/c mice (Fig. 2A, middle). We next examined the role of Exo-srIκB in survival using a model of CLP-induced sepsis as a standardized murine model of intra-abdominal sepsis. The animals survived the 7-day monitoring period, indicating that Exo-srIκB provides lasting protection against sepsis mortality (Fig. 2A, bottom). To further investigate whether Exo-srIκB treatment alleviated the inflammation induced by sepsis, enzyme-linked immunosorbent assay (ELISA) was used to determine the concentrations of key inflammation factors in the serum. We observed significant reductions in the expression levels of the proinflammatory cytokines TNF-α, IL-1β, and IL-6, as well as the C-C Motif Chemokine Ligand 4 (CCL4), in the Exo-srIκB treatment group with LPS-induced sepsis (Fig. 2B, top). We also observed that serum levels of TNF-α

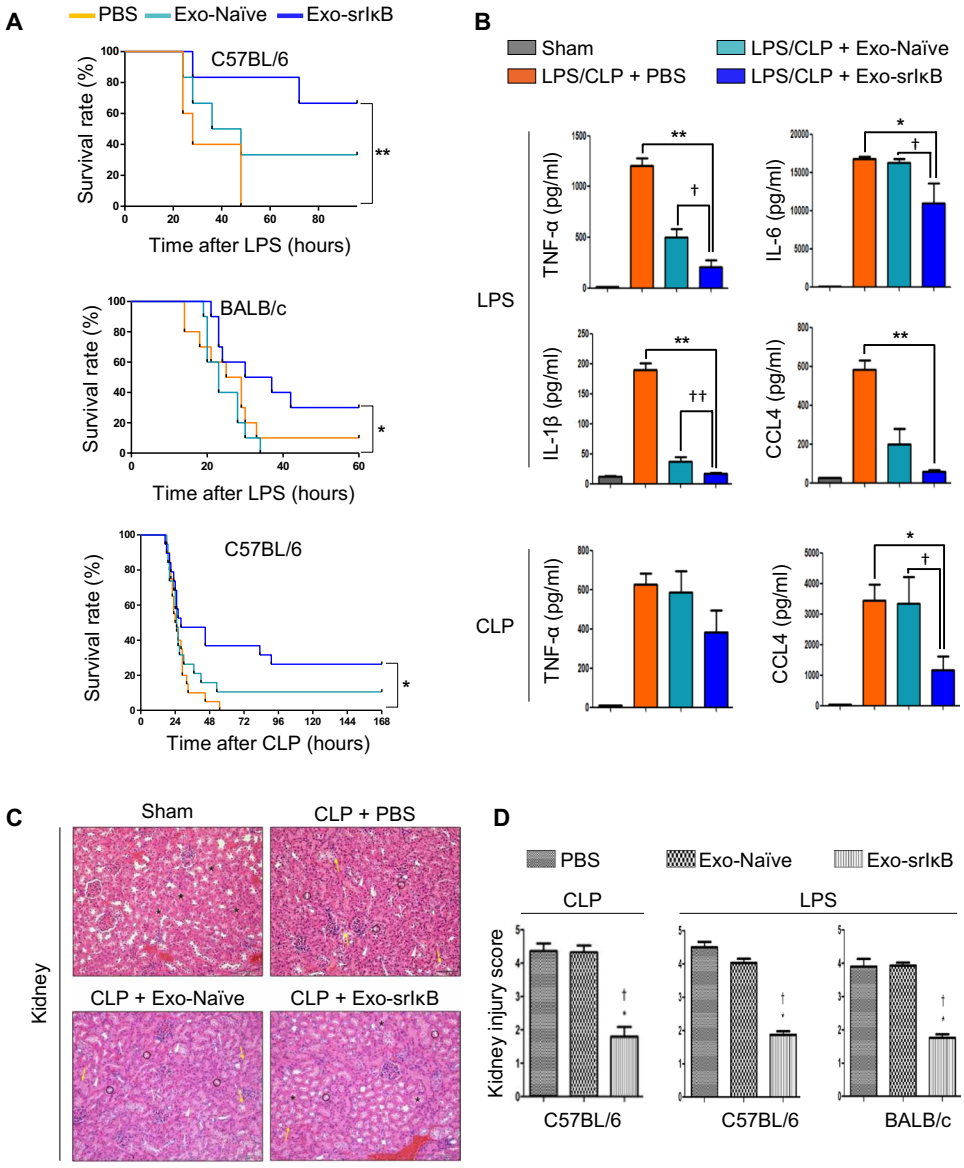

Fig. 2. The protective effects of Exo-srIκB in endotoxemia and CLP-induced sepsis. (**A**) Survival curves of phosphate-buffered saline (PBS)–, Exo-Naïve–, and Exo-srIκB–treated septic mice. LPS C57BL/6 mice ($n = 5$ to 6 per group), LPS BALB/c mice ($n = 10$ per group), and CLP C57BL/6 mice ($n = 14$ to 15 per group). $^{**}P < 0.01$ and $^{*}P < 0.05$ compared with the PBS-treated sepsis group. (**B**) Levels of TNF-α, IL-6, IL-1β, and CCL4/macrophage inflammatory protein-1β in the plasma of exosome-treated mice were measured 24 hours after LPS injection or CLP. $^{**}P < 0.01$ and $^{*}P < 0.05$ compared with the PBS-treated sepsis group. †$P < 0.05$ compared with the Exo-Naïve–treated sepsis group. (**C**) Representative images of cortical tubular cells in kidney sections from sham, CLP with PBS, CLP with Exo-Naïve, and CLP with Exo-srIκB mice. Normal brush border (*) of proximal tubules or loss of brush border (○), chromatin condensation (white arrows), denuded basement membrane (white arrow heads), and vacuolization (yellow arrows). Scale bars, 100 μM. (**D**) Pathological kidney injury scores of representative kidney samples of each group. $^{*}P < 0.05$ compared with the PBS-treated sepsis group. †$P < 0.05$ compared with the Exo-Naïve–treated sepsis group. GFP, green fluorescent protein; GAPDH, glyceraldehyde-3-phosphate dehydrogenase.

and CCL4 in the CLP group were significantly higher than those in sham-operation control mice but were not elevated in mice treated with both CLP and Exo-srIκB (Fig. 2B, bottom). These results suggest that Exo-srIκB alleviates inflammation induced by LPS or CLP and protects septic mice against the acute inflammatory process.

Numerous studies have shown that acute kidney injury (AKI) is a frequent and serious complication of sepsis, occurring in 50% or more cases, and is associated with very high mortality (*21*). To determine the role of Exo-srIκB in CLP-induced AKI in the septic mouse model, renal histological examination was performed. In comparison with those that underwent a sham operation, the renal tubular cells of mice treated with phosphate-buffered saline (PBS) and Exo-Naive mice showed significant damage in terms of vacuolization, loss of the brush border, and nuclear condensation of tubular epithelial cells (Fig. 2C). Notably, Exo-srIκB treatment markedly decreased damage to tubular areas, preserving proximal tubules and demonstrating the therapeutic potential of Exo-srIκB for sepsis-induced renal injury. These results are consistent with those for LPS-induced AKI (fig. S2B). We further quantified the severity of histological kidney damage and found that Exo-srIκB treatment significantly reduced the injury score by 50% in both sepsis models (Fig. 2D). Exo-srIκB ameliorated degenerative changes in the renal tubules, although some damaged areas were present. These data suggest the critical importance of Exo-srIκB in improving renal physiological structure and function in septic mice.

Biodistribution of exosomes after LPS injection

Next, we investigated the changes in exosome biodistribution in the LPS-injected septic mouse model. The in vivo biodistribution was analyzed using a custom-made intravital video-rate laser scanning confocal microscopy system (*22*). mCLING fluorescence dye–labeled exosomes were intravenously injected into $LysM^{gfp/+}$ transgenic C57BL/6 mice that had also been injected with anti-Ly6G antibody to visualize neutrophils [green fluorescent protein (GFP) and Alexa Fluor 555] and macrophages (GFP). We observed that most exosomes were taken up by neutrophils and macrophages rapidly, i.e., within a few minutes of intravenous exosome injection (Fig. 3A and movie S1).

Exosomes were delivered mainly to the neutrophils of the liver (Fig. 3B), and we observed increased recruitment of neutrophils and macrophages, as well as increased uptake of exosomes, in the spleens of LPS-induced mice (Fig. 3C). mCLING-labeled exosomes were also delivered to neutrophils in the kidneys of LPS-injected mice (fig. S3A). These observations suggest that therapeutic exosomes were successfully delivered to target neutrophils and macrophages within 30 min in the septic mouse model.

Exo-srIκB alleviates inflammation associated with sepsis

Next, we identified the target specificity and efficiency of Exo-srIκB in vitro. Exo-srIκB, but not Exo-Naïve, significantly blocked TNF-α–induced NF-κB activation in an HEK293 cell stably expressing an NF-κB luciferase reporter gene (Fig. 4A). Increasing doses of Exo-srIκB decreased NF-κB reporter activity in a dose-dependent manner, indicating that srIκB released from exosomes prevents NF-κB transcriptional activity (Fig. 4B).

Among all sepsis-responsive cells, monocytes/macrophages play the most critical role in promoting the immune response (*23*), and depletion of these cells in septic mice increases mortality (*24*). THP-1 cells are widely used to represent monocytes in cell culture models. When THP-1 cells were stimulated with LPS, treatment with Exo-srIκB led to decreased secretion of the inflammatory cytokines TNF-α and monocyte chemoattractant protein-1 (MCP-1), which are under NF-κB transcriptional control, compared with Exo-Naïve (Fig. 4C). We also compared the effects of Exo-srIκB with those of the commonly used NF-κB inhibitor JSH-23, which interferes with the binding of NF-κB to its target DNA (*25*). Our data showed that Exo-srIκB and JSH-23 had comparable effects with respect to inhibiting LPS-induced NF-κB activation and cytokine production in THP-1 cells (Fig. 4C, lane 4 versus lane 6).

Sepsis is characterized by monocyte adherence to the endothelium. Under normal conditions, endothelial cells are quiescent and do not interact with monocytes. However, in an inflammatory environment, activated endothelial cells express adhesion molecules, such as intercellular cell adhesion molecule-1 (ICAM-1), which bind to monocytes. The expression of adhesion molecules is widely considered to be activated during the development of sepsis (*26*). To explore the effect of Exo-srIκB on the expression of cell adhesion molecules in human umbilical vein endothelial cells (HUVECs), we first examined whether Exo-srIκBs are internalized in the cells. mCLING-labeled Exo-srIκBs were detectable in HUVECs, with maximum internalization observed after 24 hours (Fig. 4D). We found that ICAM-1 expression in HUVECs was significantly inhibited by Exo-srIκB treatment (Fig. 4E). IL-8 and MCP-1 also triggered the migration and adhesion of monocytes to the vascular endothelium and led to extravasation of these cells into the surrounding tissues (*27*). Expression of IL-8 and MCP-1 has been observed previously in various tissues during acute inflammation caused by bacterial and viral infections and is associated with severe sepsis (*28*). We found that Exo-srIκB suppressed LPS-induced IL-8 and MCP-1 production (fig. S4A) by inhibiting NF-κB transcriptional activity in HUVECs (fig. S4B). These results suggest that Exo-srIκB reduces the NF-κB–mediated inflammatory response during sepsis.

DISCUSSION

The complex pathophysiology of sepsis, which involves multiple organ failure, hinders the development of therapeutic agents that can effectively treat all manifestations of sepsis. Nevertheless, the general consensus is that sepsis is initiated through strong activation of the innate immune system and mediated by the activation of pattern recognition receptors by pathogens, leading to activation of the complement system, the coagulation system, and the vascular endothelium (*29*). This process is followed by an immunosuppressive state, which, in turn, results in a failure to return to normal homeostasis. Therefore, innovative immunomodulatory agents that can target the root cause of sepsis are urgently needed. Here, we report the effect of Exo-srIκB on resolving inflammatory responses and reducing organ damage in a septic mouse model through inhibition of NF-κB activity. We used a recently developed technology that can load functional proteins into exosomes (EXPLOR) to generate an immunosuppressive exosome loaded with srIκB (*20*). srIκB is a nondegradable form of IκBα that prevents NF-κB from entering the nucleus and acting as a transcription factor (*14*, *15*).

Through systemic delivery of Exo-srIκB in a septic mouse model, we demonstrated that exosomes are delivered primarily to neutrophils and macrophages, which are key players in the overwhelming inflammatory response of sepsis. Our results showed that Exo-srIκB

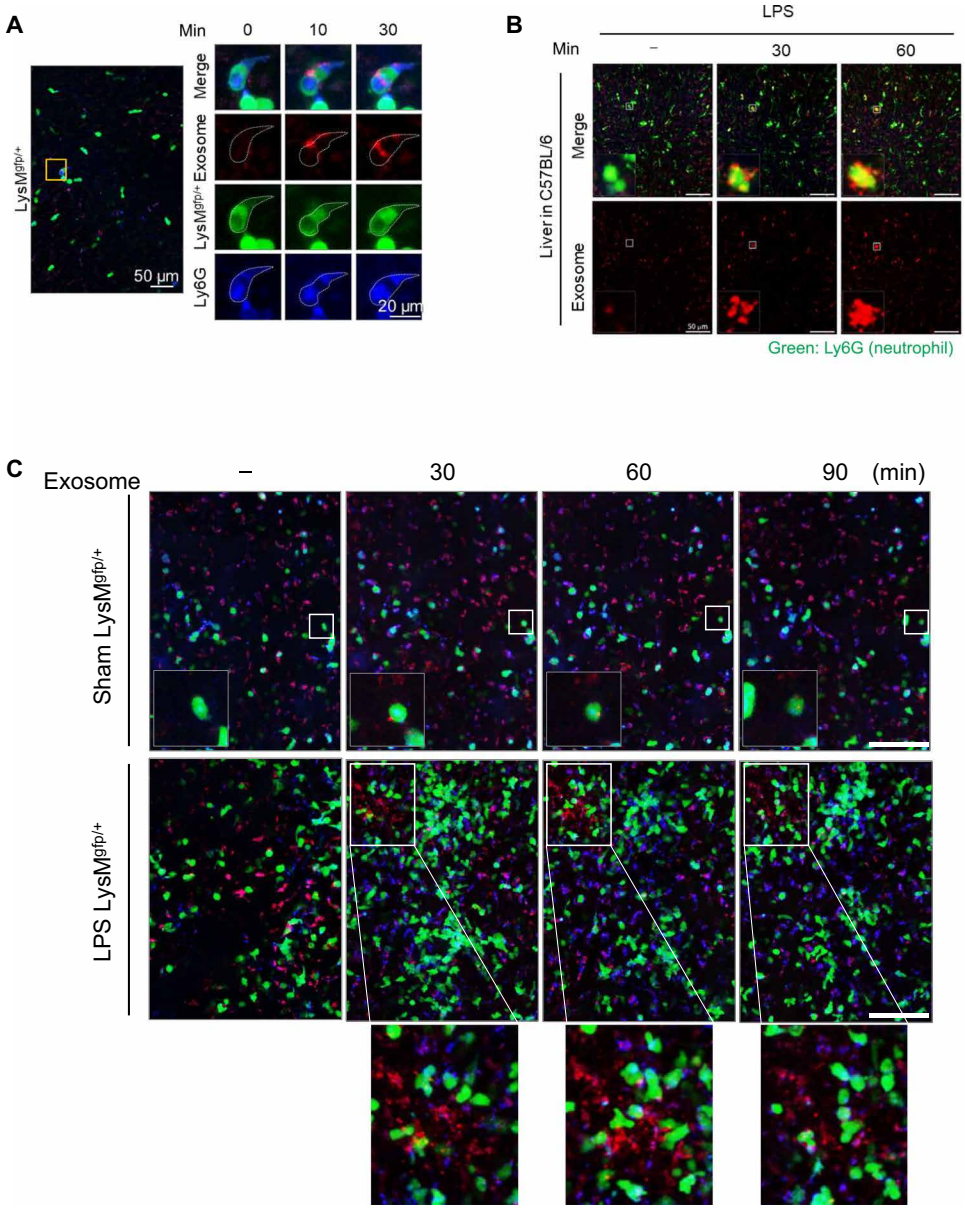

Fig. 3. The biodistribution of exosomes in LPS-injected mice. (**A**) Intravital imaging of mCLING-labeled exosome (red) uptake into neutrophils (LysM$^{gfp/+}$, green; Ly6G^{+}, blue) in the liver of sham mice. (**B**) Representative time-lapse imaging of mCLING-labeled exosomes (red) inside the Ly6G^{+} neutrophil cells (green) of the liver in LPS-treated C57BL/6 mice. (**C**) Sequential images of flowing mCLING-labeled exosomes (red) inside the spleen of sham- and LPS-treated LysM$^{gfp/+}$ mice. Elapsed time is indicated. Magenta, autofluorescence. Scale bars, 50 μm.

treatment significantly reduced proinflammatory markers such as TNF-α, IL-1β, and IL-6, but not the anti-inflammatory cytokine IL-10 (fig. S2D), in two mouse sepsis models. Even when exosomes were injected 1 hour after LPS injection, we observed a significant therapeutic effect of Exo-srIκB. Considered together with our other findings, these results show that Exo-srIκB treatment could be administered during the early phase of sepsis, before conversion to the immunosuppressive state.

Growing evidence has shown that proinflammatory cytokines play a prominent role in sepsis-induced AKI (*30*). In the present study, we successfully established a murine model of sepsis-induced AKI through CLP surgery or LPS injection. Histopathological examination showed that the glomerular structure was destroyed, renal tubular epithelial cells were degenerated, and severe intracellular edema and congestion occurred within the renal tubule in the sepsis-induced group. However, treatment with Exo-srIκB reduced the severity of lesions and limited renal injury and the infiltration of inflammatory cells.

Numerous studies have suggested that neutrophil tissue infiltration is a key process in sepsis (*31*, *32*). For example, depletion of neutrophils or inhibition of neutrophil recruitment through targeting specific adhesion molecules has been repeatedly shown to protect against tissue injury in sepsis (*33*, *34*). TNF-α and IL-1β are major mediators of the expression of chemokines such as MCP-1

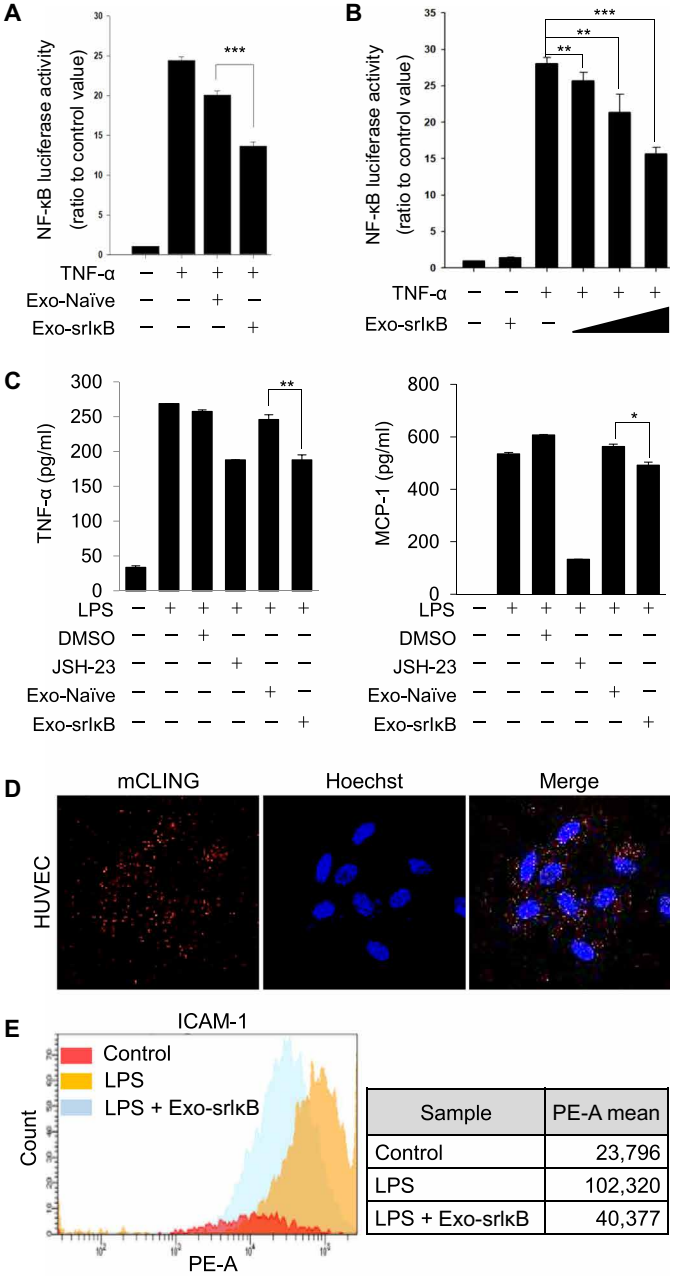

Sample	PE-A mean
Control	23,796
LPS	102,320
LPS + Exo-srIκB	40,377

Fig. 4. Inhibitory effect of Exo-srIκB on NF-κB signaling in vitro. (**A**) HEK293–NF-κB–luciferase cells (2×10^4 cells) were cultured either with Exo-Naïve or with Exo-srIκB (2×10^5 particles). After 24 hours, the cells were treated with TNF-α (0.5 ng/ml) for an additional 18 hours. Luciferase activities were measured and normalized. (**B**) Exo-srIκB dose-dependently repressed NF-κB activation in NF-κB–luciferase cells. (**C**) THP-1 cells (5×10^5 cells) were stimulated with LPS (1 μg/ml) and then treated with Exo-srIκBs (5×10^6 particles). The supernatants were collected and assayed for the production of TNF-α and MCP-1. JSH-23 (50 μM) was used as the positive control. $^{**}P < 0.01$. (**D**) Immunofluorescence of HUVECs incubated with mCLING-labeled Exo-srIκB. Representative images are shown. Nuclei were labeled with Hoechst. (**E**) HUVECs were stimulated with LPS (300 ng/ml) for 24 hours. Cells were harvested into a single-cell suspension and assessed through flow cytometry using specific phycoerythrin (PE)–conjugated antibodies against human ICAM-1. DMSO, dimethyl sulfoxide. $^{*}P < 0.05$; $^{**}P < 0.01$; $^{***}P < 0.001$.

and IL-8, which are important chemoattractants for neutrophils and monocytes/macrophages during inflammation. These chemokines could initiate local infiltration of monocytes/macrophages after their activation. In HUVECs, Exo-srIκB could attenuate LPS-induced release of MCP-1 and IL-8, in turn inhibiting the infiltration of monocytes/macrophages. Our data are consistent with the results obtained from in vivo studies. We found that treatment with Exo-srIκB greatly decreased neutrophil infiltration in the spleen, kidney, and liver of septic animal models (fig. S2C). In light of the important role of neutrophils in the pathophysiology of sepsis (*31*, *32*), the tissue-protective effect of Exo-srIκB might be related, at least in the kidney, to decreased infiltration of neutrophils. The spleen showed a higher level of neutrophils compared with other organs, such as the kidney and liver, suggesting that proinflammatory cytokines may arise in the spleen and subsequently affect other organs.

Most genes encoding proinflammatory cytokines are under the control of NF-κB, which is one of the most important transcription factors in the LPS-induced septic inflammation response (*35*). In this study, we examined the expression of NF-κB–responsive reporter proteins and measured p65 translocation in the presence and absence of Exo-srIκB treatment. As expected, our results showed that Exo-srIκBs inhibit NF-κB signal activation by blocking nuclear translocation of NF-κB subunit p65.

Current conventional strategies to deliver the therapeutic proteins include enveloping the proteins within synthetic nanoparticles (*36*). The most preferred protein delivery systems are liposomes and polymeric nanoparticles (PNPs). A liposome is a synthetic vesicle with a phospholipid membrane that self-assembles into various sizes and shapes in an aqueous environment. A PNP is a solid colloidal particle with the size between 10 and 1000 nm and is made up of biodegradable polymers, in which the cargo proteins can be entrapped, encapsulated, or attached to a nanoparticle matrix (*37*). However, liposomes tend to fuse or aggregate with each other, resulting in immature release of cargo over time (*38*). PNPs may have better stability than liposomes, but their biocompatibility and long-term potential safety are still a concern. In addition, encapsulating proteins to liposomes and PNPs requires generation of synthetic or recombinant proteins and ex vivo encapsulation processes, whereas EXPLOR technology requires generation and maintenance of stable cells that can produce cargo-loaded exosomes via natural exosome biogenesis. In addition, exosomes have many desirable features of an ideal protein delivery system, such as biocompatibility, minimal or no inherent toxicity, long half-life in the circulation, and intrinsic ability to target tissues (*39*).

In conclusion, we used exosomes as a mechanism for therapeutic delivery of immunosuppressive proteins in a septic mouse model. Exosomes are a promising vehicle for intracellular delivery of srIκB and constitute a new option for sepsis therapy; no methods of delivering immunosuppressive proteins directly into the target cells in vivo have been established previously. Our data demonstrate that Exo-srIκB acts as an inhibitor of NF-κB and can directly counteract the overwhelming inflammatory response, thus ameliorating the proinflammatory cytokine storm and subsequent organ damage.

MATERIALS AND METHODS

Animals

All animal experiments were performed in accordance with standard guidelines for the care and use of laboratory animals and were

approved by our Institutional Animal Care and Use Committee. C56BL/6, C57BL/6N, and BALB/c mice were purchased from Orientbio (Seong-Nam, Republic of Korea). LysM$^{gfp/+}$ mice intrinsically expressing GFP in neutrophils and macrophages were provided by M. Kim (University of Rochester, Rochester, NY, USA).

LPS endotoxemia model

To generate the LPS endotoxemia mouse model, LPS derived from *Escherichia coli* (Sigma-Aldrich, Milwaukee, WI, USA) was injected into male mice.

High-grade CLP sepsis model and treatment regiment

Male C57BL/6 mice purchased from Orientbio (Seongnam-si, Gyeonggi-do, Republic of Korea) were subjected to high-grade CLP at 9 to 10 weeks of age using a previously described procedure with minor modification (*40*). All mice were housed, and experiments were performed in a specific pathogen–free area of Yonsei Biomedical Research Institute, Yonsei University College of Medicine, which was certified by the Association for Assessment and Accreditation of Laboratory Animal Care International. Mice were anesthetized through intraperitoneal injection of a mixture of ketamine (80 mg/kg) and xylazine (10 mg/kg) prior to all procedures. After anesthesia, the peritoneum was opened in a sterile manner, and the cecum was ligated using 4-0 black silk thread 1 cm from the distal end and punctured with a 23-gauge needle. After puncturing, the needle was removed, and a small amount of stool was extruded through both punctures to ensure patency. Then, the cecum was placed back into the abdominal cavity, and the abdominal incision was closed with 6-0 nylon sutures, with stainless steel removable wound clips used on the skin. After this procedure, 1 ml of prewarmed saline per 20-g body weight was administered subcutaneously. Sham-treated mice underwent the same procedure except for the ligation and puncture of the cecum. After this procedure, 1.0×10^9 particles of Exo-Naïve or Exo-srIκB were administered to mice via intraperitoneal injection at 0, 6, 12, and 18 hours. As a control, an equivalent volume of PBS was injected in the same manner. We assessed the animals every 2 hours during the initial 48 hours after CLP and then every 4 hours for 5 days. Samples were collected to evaluate the outcome of the procedure within 18 hours after CLP.

Intravital imaging

A laser scanning intravital confocal microscope (IVIM Technology, Daejeon, South Korea) was used to visualize the biodistribution and antiseptic effects of Exo-srIκB. During intravital imaging, mouse body temperature was maintained at 37°C using a homoeothermic controller. Mice were anaesthetized with intramuscular injections of Zoletil (30 mg/kg) and xylazine (10 mg/kg). To access the internal organs, including the liver, spleen, and kidney, a small incision of 10 mm was made in both the skin and peritoneum. Exposed organs were kept hydrated through repeated application of saline during imaging. The biodistribution of exosomes was visualized through wide-area z-stack imaging before and after the injection of Exo-Naïve or Exo-srIκB. To fluorescently label neutrophils of C57BL/6N mice in vivo, anti-Ly6G antibody (BD Bioscience, San Jose, CA, USA) conjugated with Alexa Fluor 555 (A20009, Thermo Fisher Scientific, Waltham, MA, USA) was injected intravenously. Naïve or srIκB exosomes labeled with mCLING ATTO 647N (Synaptic System, Göttingen, Germany) were intravenously injected via a tail vein catheter or 31-gauge insulin syringe. To generate the sepsis model, high-dose LPS (Sigma-Aldrich, St. Louis, MO, USA) was intravenously injected 1 to 16 hours before imaging.

Histopathologic assessment of kidney injury score

Formalin-fixed and paraffin-embedded kidney tissue samples were stained with hematoxylin and eosin and examined to assess the degree of kidney injury. To examine histologic changes in an objective manner, cortical areas were subjected to kidney injury evaluation by two pathologists (E.S.C. and J.I.Y.) in a blinded manner. Kidney injury was scored according to the percentage of damaged tubules among total tubules: 0, normal; 1, <25% damage; 2, 25 to 50% damage; 3, 50 to 75% damage; 4, 75 to 90% damage; and 5, >90% damage. Histological criteria for injured tubules were loss of the tubular brush border, vacuolization, chromatin condensation, and denuded tubular basement membrane. Renal tubules in five randomly selected high-power fields, typically including 50 to 100 tubules, were evaluated and scored.

Cell culture

HUVECs were purchased from the American Type Culture Collection (ATCC; Manassas, VA, USA) and cultured in F-12 K medium (ATCC) containing 10% fetal bovine serum (FBS; Atlas Biologicals, Fort Worth, CO, USA), heparin (Sigma-Aldrich), endothelial cell growth supplement (BD Biosciences), and 1% penicillin/streptomycin (Thermo Fisher Scientific). HUVECs between the third and sixth passages were used in all experiments. Human monocytes (THP-1) were purchased from ATCC and cultured in RPMI 1640 medium (WELGENE, Daegu, Republic of Korea) with 10% FBS, 1% penicillin/streptomycin, and 0.05 mM 2-mercaptoethanol (Sigma-Aldrich).

Confocal microscopy

For exosome uptake analysis, exosomes were diluted in 0.5 ml of Dulbecco's PBS (DPBS). Subsequently, the suspension was incubated with 647N-labeled mCLING ATTO (Synaptic System) according to the manufacturer's instructions. Then, a pellet of the mixture was obtained through centrifugation, and 300 μl of the resuspended pellet was incubated with the HUVECs. After 24 hours, cells were washed with DPBS and fixed in 4% paraformaldehyde solution. Hoechst was used for nuclear staining. Images were recorded using a Zeiss 710 confocal microscope (Zeiss, Oberkochen, Germany).

Luciferase assay

HEK293 cells were stably transfected with a luciferase reporter construct regulated under the NF-κB response element (SL-0012, Signosis, Santa Clara, CA, USA) and grown according to the manufacturer's instructions. Cells were treated with exosomes for 24 hours at 37°C, and luciferase activity was measured (E1501, Promega, Madison, WI, USA) using a SpectraMax ID3 microplate reader (Molecular Devices, Sunnyvale, CA, USA).

Western blotting

Western blotting was performed as described in a previous study (*20*). Antibodies targeting the following proteins were used: IκBα (CST4812, Cell Signaling Technology, Danvers, MA, USA), p65 (CST6956S, Cell Signaling Technology), CD9 (NBP2-22187, Novus Biologicals, Centennial, CO, USA), CD63 (EXOAB-CD63A-1, SBI, Tokyo, Japan), TSG101 (ab228013, Abcam, Cambridge, UK), GM130 (ab52649, Abcam), glyceraldehyde-3-phosphate dehydrogenase (GAPDH; sc-47724, Santa Cruz Biotechnology, Santa Cruz, CA,

USA), histone H3 (ab1791, Abcam), mCherry (ab125096, Abcam), and GFP (CST2555, Cell Signaling Technology).

Enzyme-linked immunosorbent assays

The TNF-α, IL-8, and MCP-1 levels in supernatants collected from THP-1 and HUVEC cultures were measured using commercial ELISA kits (R&D Systems, Minneapolis, MN, USA), and NF-κB activity in HUVECs was measured using the Trans AM NF-κB p65 Kit (Active Motif, Carlsbad, CA, USA). TNF-α, CCL-4/macrophage inflammatory protein (MIP)-1β, IL-6, and IL-1β levels in mouse plasma collected through cardiac puncture at the indicated time points after the high-grade CLP procedure were measured using the Mouse Magnetic Luminex Screening Assay Kit (R&D Systems). The assay was performed according to the manufacturer's instructions. All samples and standards were assayed in duplicate using the Luminex 200TM System (Merck Millipore, Darmstadt, Germany). To measure serum TNF-α, IL-1β, IL-6, and CCL4 at the indicated time points, blood samples were collected through cardiac puncture after the LPS endotoxemia procedure, allowed to clot for 2 hours at room temperature, and then centrifuged at 2000*g* for 20 min at 4°C.

Flow cytometry

The levels of surface markers expressed on HUVECs were assessed using flow cytometry. The cells were separated and harvested through centrifugation, labeled with phycoerythrin (PE)–conjugated antibodies specific for human ICAM-1 (BD Biosciences) on ice for 30 min in the dark, and then washed extensively. All samples were analyzed with a BD Celesta flow cytometer (BD Biosciences). The data were analyzed using BD FACSDiva software. PE-conjugated antibodies specific to IgG1κ (BD Biosciences) were used as the isotype control.

Isolation of exosomes

To produce Exo-srIκB, the stable cells were seeded into T175 flasks. After 1 day, the medium was carefully removed, the cells were rinsed with PBS, and exosome-depleted medium was added. Then, the cells were exposed to continuous blue light illumination from a 460-nm light emitting diode in a CO_2 incubator. After 72 hours, the cell culture supernatant was harvested and centrifuged at 1000*g* for 15 min to remove cells and cell debris and then filtered through a 0.22-μm polyethersulfone filter to remove large particles. The exosomes were isolated using molecular weight cutoff–based membrane filtration. The isolated exosomes were purified through SEC.

Transmission electron microscopy

Extracellular vesicles (EVs) were evaluated morphologically through negative staining. First, 5 μl of EV suspended in PBS was loaded onto glow-discharged carbon-coated copper grids (Electron Microscopy Sciences, Hatfield, PA, USA). After sample adsorption for 3 to 5 s, the grid was blotted with filter paper and stained with 2% uranyl acetate. Next, samples were dried for 20 s using a dryer. EVs were viewed with Tecnai G2 Retrofit (FEI Company, Hillsboro, OR, USA) at a voltage of 200 kV.

Nanoparticle trafficking analysis

A Zetaview instrument (PMX120, Particle Metrix, München, Germany) was used to analyze EV particle numbers and size distribution. Particle number was calculated from the rate of Brownian motion, and size was determined using the two-dimensional Stokes-Einstein equation based on the velocity of particle movement. All samples were diluted in 0.2-μm filtered PBS between 1:100 and 1:10,000. EV concentrations were measured on the basis of counts of 50 to 200 particles per frame. For each measurement, two cycles of scanning at 11 cell positions were performed with the following settings: focus, autofocus; camera sensitivity for all samples, 78.0; shutter, 70; and cell temperature, 25°C. The EV concentration was expressed in particle numbers per milliliter (pn/ml).

Statistical analysis

Values are presented as mean ± SEM. Statistical differences between means were determined using the unpaired two-tailed Student's *t* test or Mann-Whitney test, as appropriate. Kaplan-Meier survival plots and log-rank tests were used to compare survival results among treatment groups. Statistical significance was set at $P < 0.05$ or $P < 0.01$.

SUPPLEMENTARY MATERIALS

Supplementary material for this article is available at http://advances.sciencemag.org/cgi/content/full/6/15/eaaz6980/DC1

View/request a protocol for this paper from *Bio-protocol*.

REFERENCES AND NOTES

1. N. P. Boeddha, L. J. Schlapbach, G. J. Driessen, J. A. Herberg, I. Rivero-Calle, M. Cebey-López, D. S. Klobassa, R. Philipsen, R. de Groot, D. P. Inwald, S. Nadel, S. Paulus, E. Pinnock, F. Secka, S. T. Anderson, R. S. Agbeko, C. Berger, C. G. Fink, E. D. Carrol, W. Zenz, M. Levin, M. van der Flier, F. Martinón-Torres, J. A. Hazelzet, M. Emonts; EUCLIDS consortium, Mortality and morbidity in community-acquired sepsis in European pediatric intensive care units: A prospective cohort study from the European childhood life-threatening infectious disease study (EUCLIDS). *Crit. Care* **22**, 143 (2018).
2. M. Mitka, Drug for severe sepsis is withdrawn from market, fails to reduce mortality. *JAMA* **306**, 2439–2440 (2011).
3. M. Bosmann, P. A. Ward, The inflammatory response in sepsis. *Trends Immunol.* **34**, 129–136 (2013).
4. R. S. Hotchkiss, I. E. Karl, The pathophysiology and treatment of sepsis. *N. Engl. J. Med.* **348**, 138–150 (2003).
5. A. Iwasaki, R. Medzhitov, Toll-like receptor control of the adaptive immune responses. *Nat. Immunol.* **5**, 987–995 (2004).
6. R. Medzhitov, Recognition of microorganisms and activation of the immune response. *Nature* **449**, 819–826 (2007).
7. J. G. Kupfner, J. J. Arcaroli, H.-K. Yum, S. G. Nadler, K.-Y. Yang, E. Abraham, Role of NF-κB in endotoxemia-induced alterations of lung neutrophil apoptosis. *J. Immunol.* **167**, 7044–7051 (2001).
8. H. H. Lee, H. Dadgostar, Q. Cheng, J. Shu, G. Cheng, NF-κB-mediated up-regulation of Bcl-x and Bfl-1/A1 is required for CD40 survival signaling in B lymphocytes. *Proc. Natl. Acad. Sci. U.S.A.* **96**, 9136–9141 (1999).
9. J. H. Choi, S. H. Park, J.-K. Jung, W.-J. Cho, B. Ahn, C.-Y. Yun, Y. P. Choi, J. H. Yeo, H. Lee, J. T. Hong, S.-B. Han, Y. Kim, Caffeic acid cyclohexylamide rescues lethal inflammation in septic mice through inhibition of IκB kinase in innate immune process. *Sci. Rep.* **7**, 41180 (2017).
10. M. Sheehan, H. R. Wong, P. W. Hake, V. Malhotra, M. O'Connor, B. Zingarelli, Parthenolide, an inhibitor of the nuclear factor-κB pathway, ameliorates cardiovascular derangement and outcome in endotoxic shock in rodents. *Mol. Pharmacol.* **61**, 953–963 (2002).
11. D. Altavilla, G. Squadrito, L. Minutoli, B. Deodato, A. Bova, A. Sardella, P. Seminara, M. Passaniti, G. Urna, S. F. Venuti, A. P. Caputi, F. Squadrito, Inhibition of nuclear factor-κB activation by IRFI 042, protects against endotoxin-induced shock. *Cardiovasc. Res.* **54**, 684–693 (2002).
12. F. J. Oliver, J. Ménissier-de Murcia, C. Nacci, P. Decker, R. Andriantsitohaina, S. Muller, G. de la Rubia, J. C. Stoclet, G. de Murcia, Resistance to endotoxic shock as a consequence of defective NF-κB activation in poly (ADP-ribose) polymerase-1 deficient mice. *EMBO J.* **18**, 4446–4454 (1999).
13. S. C. Gupta, C. Sundaram, S. Reuter, B. B. Aggarwal, Inhibiting NF-κB activation by small molecules as a therapeutic strategy. *Biochim. Biophys. Acta* **1799**, 775–787 (2010).
14. D. J. Van Antwerp, I. M. Verma, Signal-induced degradation of IκBα: Association with NF-κB and the PEST sequence in IκBα are not required. *Mol. Cell. Biol.* **16**, 6037–6045 (1996).
15. C. Jobin, A. Panja, C. Hellerbrand, Y. Iimuro, J. Didonato, D. A. Brenner, R. B. Sartor, Inhibition of proinflammatory molecule production by adenovirus-mediated expression

of a nuclear factor κB super-repressor in human intestinal epithelial cells. *J. Immunol.* **160**, 410–418 (1998).
16. L. Alvarez-Erviti, Y. Seow, H. Yin, C. Betts, S. Lakhal, M. J. Wood, Delivery of siRNA to the mouse brain by systemic injection of targeted exosomes. *Nat. Biotechnol.* **29**, 341–345 (2011).
17. S. Kamerkar, V. S. LeBleu, H. Sugimoto, S. Yang, C. F. Ruivo, S. A. Melo, J. J. Lee, R. Kalluri, Exosomes facilitate therapeutic targeting of oncogenic KRAS in pancreatic cancer. *Nature* **546**, 498–503 (2017).
18. T. A. Shtam, R. A. Kovalev, E. Y. Varfolomeeva, E. M. Makarov, Y. V. Kil, M. V. Filatov, Exosomes are natural carriers of exogenous siRNA to human cells in vitro. *Cell Commun. Signal.* **11**, 88 (2013).
19. M. Colombo, G. Raposo, C. Théry, Biogenesis, secretion, and intercellular interactions of exosomes and other extracellular vesicles. *Annu. Rev. Cell Dev. Biol.* **30**, 255–289 (2014).
20. N. Yim, S. W. Ryu, K. Choi, K. R. Lee, S. Lee, H. Choi, J. Kim, M. R. Shaker, W. Sun, J. H. Park, D. Kim, W. D. Heo, C. Choi, Exosome engineering for efficient intracellular delivery of soluble proteins using optically reversible protein-protein interaction module. *Nat. Commun.* **7**, 12277 (2016).
21. S. Uchino, J. A. Kellum, R. Bellomo, G. S. Doig, H. Morimatsu, S. Morgera, M. Schetz, I. Tan, C. Bouman, E. Macedo, N. Gibney, A. Tolwani, C. Ronco; Beginning and Ending Supportive Therapy for the Kidney (BEST Kidney) Investigators, Acute renal failure in critically ill patients: A multinational, multicenter study. *JAMA* **294**, 813–818 (2005).
22. P. Kim, M. Puoris'haag, D. Côté, C. P. Lin, S. H. Yun, In vivo confocal and multiphoton microendoscopy. *J. Biomed. Opt.* **13**, 010501 (2008).
23. D. K. Dalton, S. Pitts-Meek, S. Keshav, I. S. Figari, A. Bradley, T. A. Stewart, Multiple defects of immune cell function in mice with disrupted interferon-gamma genes. *Science* **259**, 1739–1742 (1993).
24. T. Traeger, W. Kessler, A. Hilpert, M. Mikulcak, M. Entleutner, P. Koerner, A. Westerholt, K. Cziupka, N. van Rooijen, C. D. Heidecke, S. Maier, Selective depletion of alveolar macrophages in polymicrobial sepsis increases lung injury, bacterial load and mortality but does not affect cytokine release. *Respiration* **77**, 203–213 (2009).
25. H.-M. Shin, M.-H. Kim, B. H. Kim, S.-H. Jung, Y. S. Kim, H. J. Park, J. T. Hong, K. R. Min, Y. Kim, Inhibitory action of novel aromatic diamine compound on lipopolysaccharide-induced nuclear translocation of NF-κB without affecting IκB degradation. *FEBS Lett.* **571**, 50–54 (2004).
26. R. Zonneveld, R. Martinelli, N. I. Shapiro, T. W. Kuijpers, F. B. Plötz, C. V. Carman, Soluble adhesion molecules as markers for sepsis and the potential pathophysiological discrepancy in neonates, children and adults. *Crit. Care* **18**, 204 (2014).
27. R. E. Gerszten, E. A. Garcia-Zepeda, Y.-C. Lim, M. Yoshida, H. A. Ding, M. A. Gimbrone Jr., A. D. Luster, F. W. Luscinskas, A. Rosenzweig, MCP-1 and IL-8 trigger firm adhesion of monocytes to vascular endothelium under flow conditions. *Nature* **398**, 718–723 (1999).
28. N. Mukaida, A. Harada, K. Matsushima, Interleukin-8 (IL-8) and monocyte chemotactic and activating factor (MCAF/MCP-1), chemokines essentially involved in inflammatory and immune reactions. *Cytokine Growth Factor Rev.* **9**, 9–23 (1998).
29. T. van der Poll, F. L. van de Veerdonk, B. P. Scicluna, M. G. Netea, The immunopathology of sepsis and potential therapeutic targets. *Nat. Rev. Immunol.* **17**, 407–420 (2017).
30. S. Dirkes, Sepsis and inflammation: Impact on acute kidney injury. *Nephrol. Nurs. J.* **40**, 125–132 (2013).
31. G. Drifte, I. Dunn-Siegrist, P. Tissières, J. Pugin, Innate immune functions of immature neutrophils in patients with sepsis and severe systemic inflammatory response syndrome. *Crit. Care Med.* **41**, 820–832 (2013).
32. K. A. Brown, S. D. Brain, J. D. Pearson, J. D. Edgeworth, S. M. Lewis, D. F. Treacher, Neutrophils in development of multiple organ failure in sepsis. *Lancet* **368**, 157–169 (2006).
33. H. Hartman, A. Abdulla, D. Awla, B. Lindkvist, B. Jeppsson, H. Thorlacius, S. Regnèr, P-selectin mediates neutrophil rolling and recruitment in acute pancreatitis. *Br. J. Surg.* **99**, 246–255 (2012).
34. J. L. Frossard, A. Saluja, L. Bhagat, H. S. Lee, M. Bhatia, B. Hofbauer, M. L. Steer, The role of intercellular adhesion molecule 1 and neutrophils in acute pancreatitis and pancreatitis-associated lung injury. *Gastroenterology* **116**, 694–701 (1999).
35. S. F. Liu, A. B. Malik, NF-κB activation as a pathological mechanism of septic shock and inflammation. *Am. J. Physiol. Lung Cell. Mol. Physiol.* **290**, L622–L645 (2006).
36. R. van der Meel, M. H. Fens, P. Vader, W. W. van Solinge, O. Eniola-Adefeso, R. M. Schiffelers, Extracellular vesicles as drug delivery systems: Lessons from the liposome field. *J. Control. Release* **195**, 72–85 (2014).
37. K. S. Soppimath, T. M. Aminabhavi, A. R. Kulkarni, W. E. Rudzinski, Biodegradable polymeric nanoparticles as drug delivery devices. *J. Control. Release* **70**, 1–20 (2001).
38. C. K. Haluska, K. A. Riske, V. Marchi-Artzner, J.-M. Lehn, R. Lipowsky, R. Dimova, Time scales of membrane fusion revealed by direct imaging of vesicle fusion with high temporal resolution. *Proc. Natl. Acad. Sci. U.S.A.* **103**, 15841–15846 (2006).
39. D. Ha, N. Yang, V. Nadithe, Exosomes as therapeutic drug carriers and delivery vehicles across biological membranes: Current perspectives and future challenges. *Acta pharm. Sin. B* **6**, 287–296 (2016).
40. D. Rittirsch, M. S. Huber-Lang, M. A. Flierl, P. A. Ward, Immunodesign of experimental sepsis by cecal ligation and puncture. *Nat. Protoc.* **4**, 31–36 (2009).

Acknowledgments: We thank all members of ILIAS Corporation for the discussion and technical support. **Funding:** This research was supported by Basic Science Research Program through the National Research Foundation (NRF) of Korea funded by the Ministry of Education (NRF- 2017R1D1A1B03034177) and a faculty research grant of Yonsei University College of Medicine (6-2019-0078). **Author contributions:** K.Cho., C.C., K.Chu., and E.-C.S. conceived and designed the project. E.-C.S., K.Chu., K.Cho., J.I.Y., T.-H.Y., and P.K. supervised and developed the study. H.C. and Y.K. wrote the manuscript. H.C., Y.K., A.M., J.H., Y.N.K., J.H.S., S.K., N.H.K., E.S., and K.Chu. performed the experiments and analyzed the data. **Competing interests:** C.C., K.Cho., and H.C. are inventors of a patent related to this work filed by ILIAS Biologics Inc. (no. KR 10-1877010). E.-C.S., K.Chu., J.I.Y., and T.-H.Y. are scientific advisory board members of ILIAS Biologics Inc. C.C. is the founder and shareholder, and K.Cho., H.C., and Y.K. are minor shareholders of ILIAS Biologics Inc. P.K. is the founder and shareholder of IVIM Technology. All other authors declare that they have no competing interests. **Data and materials availability:** All data needed to evaluate the conclusions in the paper are present in the paper and/or the Supplementary Materials. Additional data related to this paper may be requested from the authors.

Submitted 1 October 2019
Accepted 13 January 2020
Published 8 April 2020
10.1126/sciadv.aaz6980

Citation: H. Choi, Y. Kim, A. Mirzaaghasi, J. Heo, Y. N. Kim, J. H. Shin, S. Kim, N. H. Kim, E. S. Cho, J. In Yook, T.-H. Yoo, E. Song, P. Kim, E.-C. Shin, K. Chung, K. Choi, C. Choi, Exosome-based delivery of super-repressor IκBα relieves sepsis-associated organ damage and mortality. *Sci. Adv.* **6**, eaaz6980 (2020).

Exosome-based delivery of super-repressor I#B# relieves sepsis-associated organ damage and mortality

Hojun ChoiYoungeun KimAmin MirzaaghasiJaenyoung HeoYu Na KimJu Hye ShinSeonghun KimNam Hee KimEunae Sandra ChoJong In YookTae-Hyun YooEunjoo SongPilhan KimEui-Cheol ShinKyungsoo ChungKyungsun ChoiChulhee Choi

Sci. Adv., 6 (15), eaaz6980. • DOI: 10.1126/sciadv.aaz6980